

arXiv:2512.17456v1 [quant-ph] 19 Dec 2025

Single-Photon Scattering in a Waveguide Coupled to a Lossy or Gain Giant Atom

Yu Xin,¹ Jia-Ming Zhang,^{1,*} and Bing Chen^{1,†}

¹*College of Electronics and Information Engineering,*

Shandong University of Science and Technology, Qingdao 266590, Shandong, China

(Dated: December 22, 2025)

Abstract

This work investigates single-photon scattering in a one-dimensional coupled-resonator waveguide coupled to a giant atom with a complex on-site energy. Within the generalized projection operator formalism, we derive analytical expressions for the scattering coefficients. We find that a lossy giant atom absorbs the incident wave, whereas a gain giant atom not only amplifies the incident wave but also leads to scattering divergence at certain energies, corresponding to spectral singularities. We explore the critical scattering dynamics associated with these singularities, and attribute the persistent wave emission to the existence of a stationary bound state in the continuum. Due to the presence of this bound state, the conventional time-independent scattering theory proves inadequate for such a non-Hermitian system. Furthermore, we show that the system with gain always features at least one time-growing bound state, which dominates the long-time dynamics, and we verify our time-dependent theoretical predictions via numerical simulations of Gaussian wave packet scattering.

I. INTRODUCTION

Waveguide quantum electrodynamics has established a powerful framework for engineering light-matter interactions at the quantum level, offering unprecedented control over photons and quantum emitters in engineered photonic environments [1, 2]. With the advancement of microfabrication techniques, artificial quantum systems, such as superconducting qubits [3, 4], quantum dots [5, 6], and cold atoms [7, 8], can couple to a one-dimensional waveguide via multiple spatially separated points. When the separation between these coupling points becomes comparable to the wavelength, such systems are termed giant atoms [9–12]. The finite propagation time of photons between coupling points and the interference effects among multiple coupling pathways lead to considerably more complex atom-waveguide interactions compared to small atoms. It gives rise to distinct physical phenomena, including frequency-dependent decay rates [13, 14], Lamb shifts [15, 16], and non-Markovian dynamics [17–19].

For atomic systems, spontaneous emission is an inevitable process. However, its dynamics

* Email address: zhangjiaming@sdust.edu.cn

† Email address: chenbing@sdust.edu.cn

can be fundamentally controlled by modifying the local photonic density of states, or more radically, by introducing optical gain [20–24]. Such loss or gain mechanisms are naturally described within the framework of non-Hermitian Hamiltonians via complex on-site energies. Recently, there has been growing interest in the spectral singularities of non-Hermitian systems [25–28]. Distinct from exceptional points, spectral singularities correspond to divergences in the continuous spectrum of scattering systems, leading to diverging transmission and reflection coefficients under incident excitation. These singularities have been extensively studied in systems with complex potentials [29–32] and in parity-time symmetric configurations [33–37].

This paper investigates a one-dimensional coupled-resonator waveguide in which a giant atom with loss or gain is coupled at two resonator sites. The single-photon scattering properties of this system are studied within a generalized projection operator formalism. We demonstrate that introducing gain into the giant atom leads to the appearance of spectral singularities. The analysis of the full system’s bound states shows that the spectral singularity is associated with a bound state inside the waveguide continuum. In parallel, a second bound state whose norm grows exponentially in time exists and governs the long-term dynamics.

The rest of the paper is organized as follows. In Sec. II, we introduce the model and outline the projection operators formalism. In Sec. III, we derive analytical expressions for the reflection and transmission coefficients using the scattering theory and establish the condition for the emergence of spectral singularities. In Sec. IV, we analyze the bound-state spectrum, numerically simulate the scattering process of a Gaussian wave packet, and interpret the resulting probability distribution in terms of the properties of the bound states. Finally, the main conclusions are presented in Sec. V.

II. THE MODEL AND PROJECTION FORMALISM

The system comprises an infinite one-dimensional coupled-resonator waveguide and a two-level giant atom connected to the waveguide at two separate sites. The Hamiltonian H of the total system can be divided into three parts, $H = H_a + H_c + H_I$, where

$$H_a = (\omega_a + i\gamma)\sigma^+\sigma^-, \quad (1)$$

$$H_c = \omega_c \sum_j c_j^\dagger c_j - J \sum_j (c_{j+1}^\dagger c_j + c_j^\dagger c_{j+1}), \quad (2)$$

and

$$H_I = g(c_0^\dagger \sigma^- + c_N^\dagger \sigma^-) + \text{H.c.} \quad (3)$$

The Hamiltonian H_a describes a two-level giant atom with transition frequency ω_a , and σ^\pm are raising and lowering operators of the giant atom. The term $i\gamma$ denotes its loss or gain, for $\gamma < 0$ in an absorptive medium [38] or $\gamma > 0$ in an amplifying medium [39], respectively. For the waveguide Hamiltonian H_c , the resonance frequency of each cavity is ω_c , the creation and annihilation operators at site j are c_j^\dagger and c_j , and the hopping strength between neighboring sites is J . The giant atom is connected to the waveguide at two specific sites, labeled 0 and N , with an equal coupling strength g , as shown in Fig. 1.

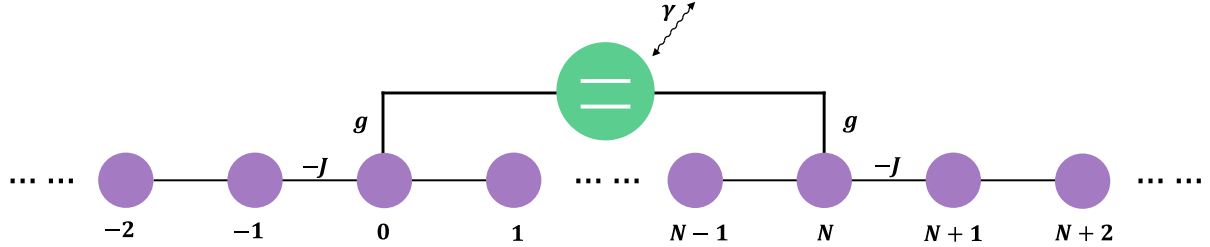


FIG. 1. Schematic diagram of a loss or gain giant atom coupled to a one-dimensional coupled-resonator waveguide modeled as a tight-binding chain.

Given the translational symmetry of the waveguide, we transform the Hamiltonian into the Bloch representation. The real-space operators of the waveguide can be expressed in terms of the continuous momentum basis via a Fourier transform:

$$c_j = \frac{1}{\sqrt{2\pi}} \int_{-\pi}^{\pi} dk e^{ikj} c_k, \quad (4)$$

where c_k is the annihilation operator for a Bloch mode with momentum k . Substituting Eq. (4) into the waveguide Hamiltonian H_c and the interaction Hamiltonian H_I , we have

$$H_c = \int_{-\pi}^{\pi} \omega_k c_k^\dagger c_k, \quad (5)$$

and

$$H_I = \frac{g}{\sqrt{2\pi}} \int_{-\pi}^{\pi} dk [(1 + e^{ikN}) \sigma^+ c_k + \text{H.c.}] . \quad (6)$$

The dispersion relation for the waveguide is $\omega_k = \omega_c - 2J \cos k$, describing an energy band located at ω_c with a width of $4J$, and the group velocity of a photon wave packet is $v_g = d\omega_k/dk = 2J \sin k$.

As we focus on the photon transport in the waveguide, the scattering problem is investigated using the projection operator formalism and an effective non-Hermitian Hamiltonian approach [40–42]. A brief overview of the method is provided below. It is always possible to subdivide the total space into two orthogonal subspaces via projection operators Q and P , which satisfy the completeness relation $Q + P = 1$ and the orthogonality condition $QP = PQ = 0$. Accordingly, the total wave function can be expressed as $|\Psi\rangle = Q|\Psi\rangle + P|\Psi\rangle = |\Psi_Q\rangle + |\Psi_P\rangle$. Applying the projectors to the left of the stationary Schrödinger equation $H|\Psi\rangle = E|\Psi\rangle$, two coupled equations that describe the mutual influence between the two subspace components yield,

$$(H_{PP} - E)|\Psi_P\rangle = -H_{PQ}|\Psi_Q\rangle, \quad (7)$$

$$(H_{QQ} - E)|\Psi_Q\rangle = -H_{QP}|\Psi_P\rangle, \quad (8)$$

where

$$H_{QQ} = QHQ, \quad H_{PP} = PHP, \quad H_{QP} = QHP, \quad H_{PQ} = PHQ. \quad (9)$$

After eliminating $|\Psi_P\rangle$, we obtain the Schrödinger equation in the Q -subspace,

$$H_{\text{eff}}(E)|\Psi_Q\rangle = E|\Psi_Q\rangle, \quad (10)$$

where the energy dependent effective Hamiltonian is

$$H_{\text{eff}}(E) = H_{QQ} + H_{QP} \frac{1}{E - H_{PP}} H_{PQ}. \quad (11)$$

It should be emphasized that $|\Psi_Q\rangle$ represents the part of the wave function residing on the Q -subspace, and is not the eigenfunction of the energy E .

III. TIME-INDEPENDENT SCATTERING THEORY IN THE PROJECTOR FORMALISM

We assume that Q -subspace is the Hilbert space of the giant atom, while the P -subspace spans the continuum of single-photon propagating modes in the waveguide. Since the giant atomic Hamiltonian (1) is non-Hermitian, the construction of the projector Q must adhere

to the general theory of non-Hermitian quantum systems. Following standard biorthogonal formulation for non-Hermitian systems [25, 43], the right eigenstate $|a\rangle$ of H_a and the corresponding right eigenstate $|a^\dagger\rangle$ of its adjoint H_a^\dagger form a complete biorthonormal basis, satisfying $\langle a^\dagger|a\rangle = 1$. The projector Q is accordingly defined as

$$Q = |a\rangle\langle a^\dagger|. \quad (12)$$

In the complementary P -subspace, the projection operator is expressed as

$$P = \int dk |k\rangle\langle k|, \quad (13)$$

with $\langle k|k'\rangle = \delta(k-k')$. Substituting the expressions (12) and (13) into Eqs. (9), we explicitly give the specific forms of the Hamiltonian components:

$$\begin{aligned} H_{QQ} &= (\omega_a + i\gamma)|a\rangle\langle a^\dagger|, \\ H_{PP} &= \int_{-\pi}^{\pi} \omega_k |k\rangle\langle k| dk, \\ H_{QP} &= \frac{g}{\sqrt{2\pi}} \int_{-\pi}^{\pi} dk (1 + e^{ikN}) |a\rangle\langle k|, \\ H_{PQ} &= \frac{g}{\sqrt{2\pi}} \int_{-\pi}^{\pi} dk (1 + e^{-ikN}) |k\rangle\langle a^\dagger|. \end{aligned} \quad (14)$$

Considering the eigenequation $H_{PP}|k\rangle = \omega_k|k\rangle$, Eq. (7) is solved to obtain the Lippmann-Schwinger equation [44],

$$|\Psi_P\rangle = |k\rangle + \frac{1}{\omega_k - H_{PP} + i\epsilon} H_{PQ} |\Psi_Q\rangle, \quad (15)$$

which describes the scattering state satisfying the outgoing wave boundary condition. Here, an infinitesimal term $i\epsilon$ (with $\epsilon > 0$) is introduced to shift the pole off the real axis into the complex plane, thereby regularizing the singularities that arise. Taking Eq. (15) into Eq. (8), we have

$$|\Psi_Q\rangle = \frac{1}{\omega_k - H_{\text{eff}}} H_{QP} |k\rangle \quad (16)$$

with the effective Hamiltonian (11) becoming

$$H_{\text{eff}}(\omega_k) = H_{QQ} + H_{QP} \frac{1}{\omega_k - H_{PP} + i\epsilon} H_{PQ}. \quad (17)$$

To simplify the analysis, we assume the resonant case $\omega_a = \omega_c$ in the following. The scattering-state wave function of the full system is given by

$$\begin{aligned} |\Psi(k)\rangle &= \left[1 + \frac{1}{\omega_k - H_{\text{eff}}(\omega_k)} H_{QP} + \frac{1}{\omega_k - H_{PP} + i\epsilon} H_{PQ} \frac{1}{\omega_k - H_{\text{eff}}(\omega_k)} H_{QP} \right] |k\rangle \\ &= \frac{g(1 + e^{ikN})}{\sqrt{2\pi}} \mathcal{R} |a\rangle + |k\rangle + \frac{g^2(1 + e^{ikN})}{2\pi} \mathcal{R} \int_{-\pi}^{\pi} \frac{1 + e^{-iqN}}{\omega_k - \omega_q + i\epsilon} |q\rangle dq, \end{aligned} \quad (18)$$

where \mathcal{R} is the inverse of $\langle a^\dagger | \omega_k - H_{\text{eff}}(\omega_k) | a \rangle$,

$$\mathcal{R} = \frac{-J \sin k}{2J^2 \sin k \cos k + i\gamma J \sin k - ig^2(e^{ikN} + 1)}, \quad (19)$$

which acts as a generalized reflection coefficient for the atomic subsystem. We can also obtain the corresponding state $|\Psi^\dagger(k)\rangle$ by replacing the Hamiltonians with their Hermitian conjugate,

$$|\Psi^\dagger(k)\rangle = \frac{g(1 + e^{-ikN})}{\sqrt{2\pi}} \mathcal{R}^* |a^\dagger\rangle + |k\rangle + \frac{g^2(1 + e^{-ikN})}{2\pi} \mathcal{R}^* \int_{-\pi}^{\pi} \frac{1 + e^{iqN}}{\omega_k - \omega_q + i\epsilon} |q\rangle dq. \quad (20)$$

In scattering theory, the S -matrix fully characterizes the scattering observables and connects the amplitudes of the incoming and outgoing channels. Based on the exact expression for the scattering state in Eq. (18), the S -matrix element can be expressed as [45]

$$\begin{aligned} S_{k'k} &= \delta(k' - k) - 2\pi i \delta(\omega_{k'} - \omega_k) \langle k' | H_{PQ} | a \rangle \mathcal{R} \langle a^\dagger | H_{QP} | k \rangle \\ &= \delta(k' - k) - \delta(\omega_{k'} - \omega_k) \frac{g^2 J \sin k (1 + e^{-ik'N}) (1 + e^{ikN})}{2i J^2 \sin k \cos k - \gamma J \sin k + g^2 (1 + e^{ikN})}. \end{aligned} \quad (21)$$

The reflection amplitude r and the transmission amplitude t correspond, respectively, to the probability amplitudes for the photon's momentum to be reversed or preserved upon interaction with the giant atom. These coefficients are extracted from the S -matrix by evaluating $S_{k'k}$ at $k' = -k$ and $k' = k$, yielding

$$r = -\frac{g^2(1 + e^{ikN})^2}{2g^2 + 2g^2 e^{ikN} - 2J\gamma \sin k + 4iJ^2 \sin k \cos k}, \quad (22)$$

$$t = 1 - \frac{g^2(1 + e^{ikN})(1 + e^{-ikN})}{2g^2 + 2g^2 e^{ikN} - 2J\gamma \sin k + 4iJ^2 \sin k \cos k}, \quad (23)$$

respectively. The same results can also be obtained by the stationary state approach, with the detailed calculation provided in Appendix A.

Figure 2 plots the reflection rate $R = |r|^2$, the transmission rate $T = |t|^2$, and their sum $R + T$ as functions of the photon energy ω_k in the waveguide for absorbing and amplifying giant atoms. From the interaction Hamiltonian (6), it follows that the giant atom decouples effectively from the waveguide for wave vectors satisfying $k = (2m + 1)\pi/N$ with integer m , irrespective of its loss or gain character. Meanwhile, the destructive interference between the two coupling points of the giant atom results in a perfect transmission $R = 0$ and $T = 1$, which can be verified from Eqs. (22) and (23). Except for these particular instances which obey the energy-flux conservation, $R + T < 1$ for $\gamma < 0$, whereas $R + T > 1$ for $\gamma > 0$.

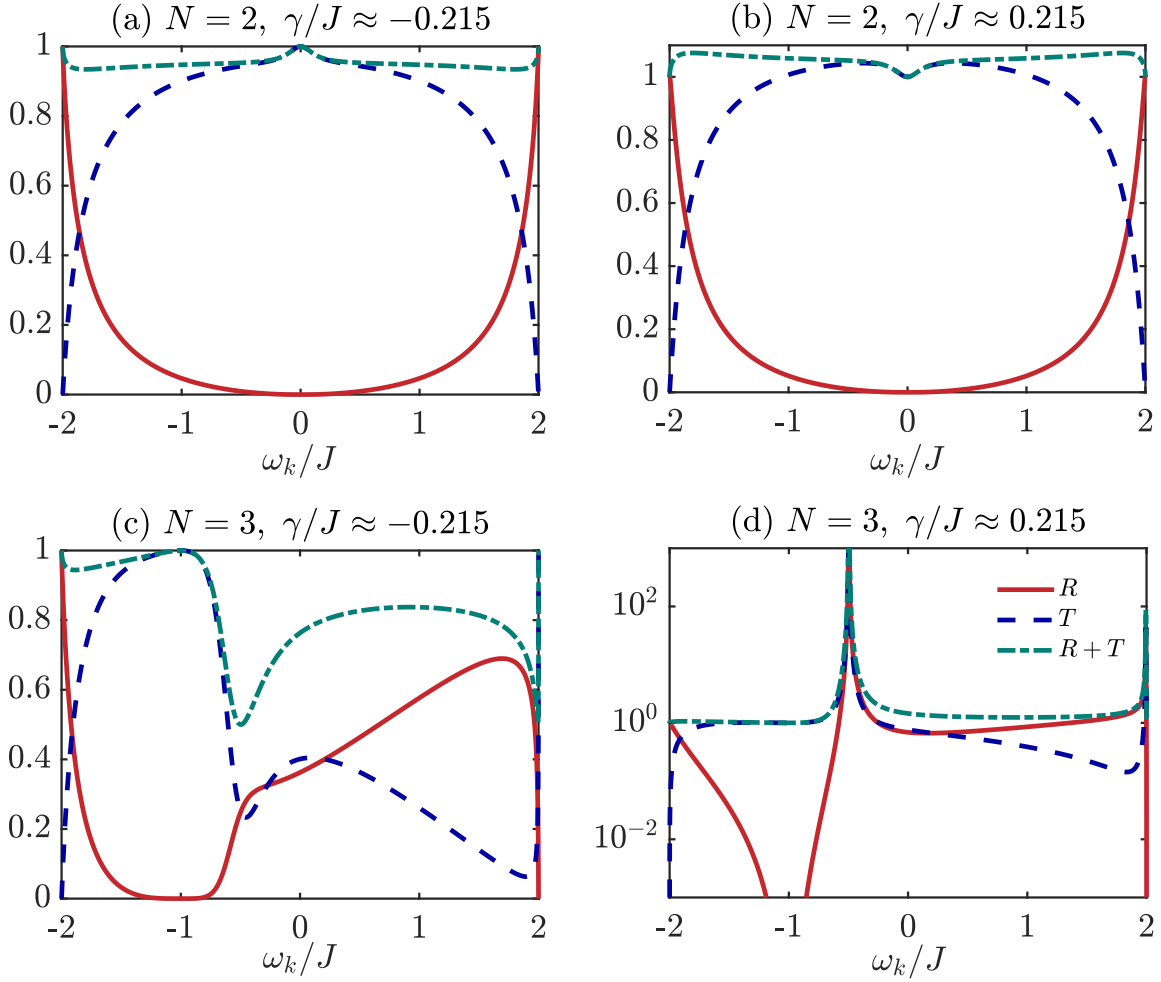


FIG. 2. Reflection rate R (red solid line), transmission rate T (blue dashed line), and their sum $R + T$ (green dotted line) as functions of the photon energy ω_k for $N = 2$ and $N = 3$ with $g/J \approx 0.812$ and $\omega_a = \omega_c = 0$. Panels (a) and (c) correspond to a loss rate $\gamma/J \approx -0.215$, while panels (b) and (d) correspond to a gain rate $\gamma/J \approx 0.215$. Only panel (d) employs a logarithmic vertical scale.

The geometric structure of the model determines the symmetry of the scattering observables, as is visually evident in Fig. 2. For even N , e.g., $N = 2$ in Fig. 2 (a) and (b), the reflection and transmission spectra are symmetric with respect to $\omega_k = 0$. This symmetry originates from the relative phase $1 + e^{\pm ikN}$ in the interaction Hamiltonian (6), which are symmetric about $k = \pi/2$ in momentum space. Consequently, the quantum interference conditions between two distinct pathways, namely direct photon propagation through the waveguide and the process of atomic absorption followed by re-emission, are symmetric with

respect to ω_k . In contrast, for odd N , the symmetry of the relative phase is broken, leading to asymmetric resonance-line shapes in the spectra, as exemplified in Fig. 2 (c) and (d) for $N = 3$.

Figure 2 (d) reveals that the reflection probability R and the transmission probability T both exhibit divergence at the energy $\omega_k/J \approx -0.496$ (corresponding to $k = 1.32$), a feature that has also been reported in small atom systems [25, 26]. Mathematically, this divergence arises from a singularity in Eqs. (22) and (23), which emerges under the following conditions:

$$\begin{cases} g^2 \sin Nk + 2J^2 \sin k \cos k = 0, \\ g^2 + g^2 \cos Nk - J\gamma \sin k = 0. \end{cases} \quad (24)$$

Notably, this condition can be satisfied only for $\gamma > 0$ when $0 < k < \pi$.

Equations (24) are also the spectral singularities conditions of the non-Hermitian model and coincide with the pole conditions of the S -matrix. The divergence of R and T implies that bidirectional outgoing waves are sustained by the gain giant atom, thereby violating the outgoing wave boundary condition for the scattering state and invalidating standard time-independent scattering theory. To analyze scattering at these singularities, we therefore turn our attention to the bound states and employ a time-dependent method to describe the wave-packet dynamics.

IV. BOUND STATES AND WAVE-PACKET DYNAMICS

Equation (10) determines the bound state projected onto the Q -subspace of the giant atom. By extending Bloch-band theory to the generalized Brillouin zone [46–48] or, equivalently, imposing Siegert boundary conditions [49], the eigenvalue takes the form $E_n = \omega_c - 2J \cos k_n$, where the wave number k_n is complex and satisfies

$$E_n = \langle a^\dagger | H_{\text{eff}} | a \rangle = \begin{cases} \omega_a + i\gamma - \frac{ig^2(1 + e^{ik_n N})}{J \sin k_n}, & \text{Im } k_n \geq 0 \\ \omega_a + i\gamma + \frac{ig^2(1 + e^{-ik_n N})}{J \sin k_n}, & \text{Im } k_n < 0 \end{cases} \quad (25)$$

In the following, we only consider $\text{Re } k_n > 0$, which corresponds to the outgoing waves and contributes to the time evolution from the initial condition [43]. The bound state for the total system thus becomes

$$|\Psi_n\rangle = \mathcal{N}_n \left[|a\rangle + \frac{g}{\sqrt{2\pi}} \int_{-\pi}^{\pi} \frac{1 + e^{-ikN}}{E_n - \omega_k + i\epsilon} |k\rangle dk \right], \quad (26)$$

and its associated state is

$$|\Psi_n^\dagger\rangle = \mathcal{N}_n^* \left[|a^\dagger\rangle + \frac{g}{\sqrt{2\pi}} \int_{-\pi}^{\pi} \frac{1 + e^{ikN}}{E_n^* - \omega_k + i\epsilon} |k\rangle dk \right], \quad (27)$$

with the normalization factor given by $\mathcal{N}_n = 1/\sqrt{1 + g^2/(2\pi) \int_{-\pi}^{\pi} dk |1 + e^{ikN}|^2 / |E_n - \omega_k|^2}$. The singularities in the denominators of Eqs. (26) and (27) are regularized by introducing infinitesimal $i\epsilon$ terms for real energies E_n , analogous to the treatment of scattering state propagators. For real eigenvalues, the real and imaginary parts of Eq. (25) are precisely equivalent to Eqs. (24). This indicates that the mathematical conditions for scattering divergence are intrinsically associated with the formation of bound states.

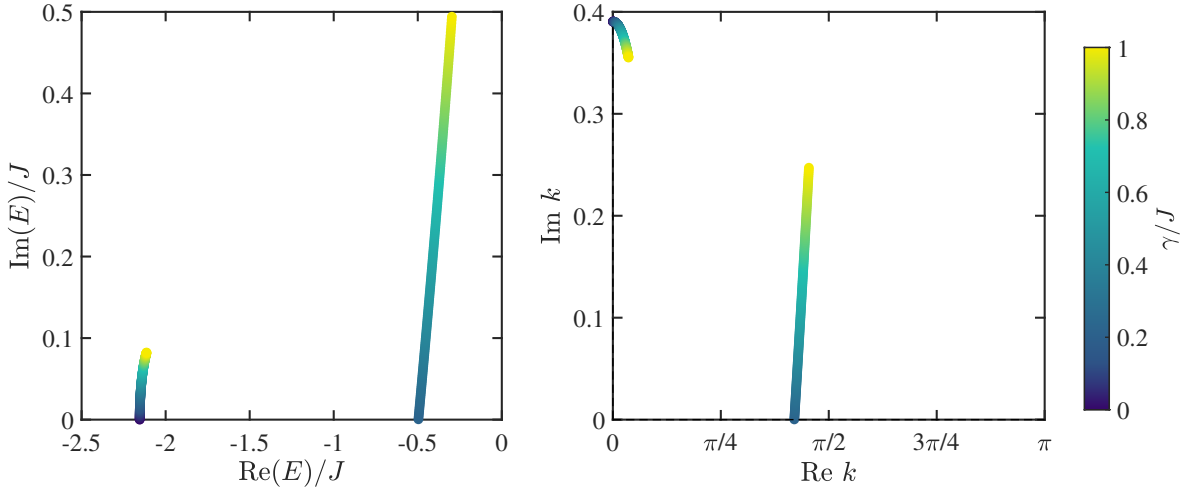


FIG. 3. Trajectories of the complex energies (left panels) and corresponding wave numbers (right panels) as functions of the gain rate γ . Other parameters are the same as Fig. 2 (c) and (d).

Given the complexity of Eq. (25), only numerical solutions are attainable. For all parameter combinations tested, we find that no numerical solution exists when $\gamma < 0$, which indicates the absence of bound states in the loss regime. Trajectories of the complex energies and the corresponding wave numbers as functions of the gain rate γ are displayed in Fig. 3. At $\gamma = 0$, a bound state with energy $E/J \approx -2.152$ exists outside the energy band $[-2J, 2J]$ and has a negligible effect on scattering. For $\gamma > 0$, points in the first quadrant of the complex k plane correspond to the first Riemann sheet of the complex E plane ($\text{Im } E > 0$) and give rise to a time-growing bound state [28]. The gain value $\gamma/J \approx 0.215$ marks a critical point beyond which a second solution emerges. At this critical gain, one eigenvalue lies

inside the energy band at $E/J \approx -0.496$, indicating the presence of two purely outgoing plane waves at both ends of the system.

Now we scrutinize the dynamical evolution of a wave packet in the waveguide after interacting with a lossy or gain giant atom. We assume that at time $t = 0$, when the wave packet encounters the giant atom, it has the following form in momentum space,

$$|\phi(0)\rangle = \int_{-\pi}^{\pi} \beta(k)|k\rangle dk. \quad (28)$$

Taking into account the energy eigenstates including both the discrete bound states and continuous scattering states, this state can be expanded as

$$|\phi(0)\rangle = \sum_n C_n |\Psi_n\rangle + \int_{-\pi}^{\pi} D(k) |\Psi(k)\rangle dk, \quad (29)$$

with

$$C_n = \langle \Psi_n^\dagger | \phi(0) \rangle = \frac{g\mathcal{N}_n}{\sqrt{2\pi}} \int_{-\pi}^{\pi} \frac{\beta(k)(1 + e^{-ikN})}{E_n - \omega_k - i\epsilon} dk, \quad (30)$$

$$D(k) = \langle \Psi^\dagger(k) | \phi(0) \rangle = \beta(k) + \frac{g^2(1 + e^{ikN})}{2\pi} \mathcal{R} \int_{-\pi}^{\pi} \frac{\beta(q)(1 + e^{-iqN})}{\omega_k - \omega_q - i\epsilon} dq, \quad (31)$$

representing the expansion coefficients at $t = 0$. The temporal evolution of the state vector $|\phi(t)\rangle$ governed by the time-dependent Schrödinger equation,

$$i\frac{d}{dt}|\phi(t)\rangle = H|\phi(t)\rangle, \quad (32)$$

yields

$$|\phi(t)\rangle = e^{-iHt}|\phi(0)\rangle = \sum_n C_n e^{-iE_n t} |\Psi_n\rangle + \int_{-\pi}^{\pi} D(k) e^{-i\omega_k t} |\Psi(k)\rangle dk. \quad (33)$$

By multiplying the position operator $\langle j |$ from the left, we project the photon wave packet into configuration space, and obtain the probability amplitude at the j -th site:

$$\langle j | \phi(t) \rangle = \sum_n C_n e^{-iE_n t} \langle j | \Psi_n \rangle + \int_{-\pi}^{\pi} D(k) e^{-i\omega_k t} \langle j | \Psi(k) \rangle dk. \quad (34)$$

According to the Riemann-Lebesgue lemma, the integral in Eq. (34) vanishes in the long-time limit [50]. Consequently, only contributions from the bound states persist. For positions outside the interval $0 < j < N$, the time evolution of the bound state is described by

$$\Psi_n(j, t) = C_n e^{-iE_n t} \langle j | \Psi_n \rangle = A_n e^{-iE_n t} e^{ik_n |j|} \quad (35)$$

with $A_n = -i\mathcal{N}_n C_n g(1 + e^{-ik_n N})/(2J \sin k_n)$, obtained from

$$\langle j|\Psi_n\rangle = \frac{\mathcal{N}_n g}{2\pi} \int_{-\pi}^{\pi} \frac{e^{ikj} + e^{ik(j-N)}}{E_n - \omega_k + i\epsilon} dk = -\frac{i\mathcal{N}_n g(1 + e^{-ik_n N})}{2J \sin k_n} e^{ik_n |j|}, \quad (36)$$

where we have used $\langle j|k\rangle = e^{ikj}/\sqrt{2\pi}$ and $\langle j|a\rangle = 0$. Equation (35) has the same form as the time evolution of the eigenstate under the Siegert boundary condition, which we established in Appendix B. It reveals that the imaginary part of wave number $\text{Im } k_n$ governs the spatial behavior and the imaginary part of the energy $\text{Im } E_n$ controls the temporal evolution. This point is revealed through the example that follows.

In order to directly visualize the time evolution of the probability distribution, we simulate the propagation of a single-photon wave packet [25, 26]. The wave packet is initialized at time $t = -t_c$ as a normalized Gaussian distribution of site occupation amplitudes,

$$\langle j|\phi(-t_c)\rangle = \pi^{-\frac{1}{4}} \alpha^{\frac{1}{2}} e^{-\frac{\alpha^2(j-j_c)^2}{2}} e^{ik_c j}. \quad (37)$$

Here, j_c and k_c represent the mean position and mean wave number of the wave packet, respectively. The wave packet is initialized sufficiently far from the coupling points ($j_c \ll 0$). Its mean group velocity is $v_c = 2J \sin k_c$, and $t_c = -j_c/v_c$ corresponds to the arrival time of the peak at the giant atom. The parameter α controls the spatial width of the wave packet, related to the momentum uncertainty through the Fourier transform relation.

Substituting the wave vector expanded in the Wannier basis, $|\phi(t)\rangle = \phi(a, t)|a\rangle + \sum_j \phi(j, t)|j\rangle$, into the time-dependent Schrödinger equation (32), a set of coupled equations for the coefficients can be derived as

$$\begin{cases} i\frac{d\phi(j, t)}{dt} = \omega_c \phi(j, t) - J[\phi(j+1, t) + \phi(j-1, t)] + g(\delta_{j,0} + \delta_{j,N})\phi(a, t), \\ i\frac{d\phi(a, t)}{dt} = -(\omega_a + i\gamma)\phi(a, t) + g[\phi(0, t) + \phi(N, t)]. \end{cases} \quad (38)$$

Equations (38) are integrated numerically using a fourth-order adaptive Runge-Kutta method. The resulting spatial profiles of the forward and backward propagating wave packets are shown in Fig. 4.

Figure 4 (a) illustrates the evolution of a wave packet for $\gamma/J \approx -0.215$. At the initial time $t = -t_c$, the momentum distribution of the wave packet is also Gaussian,

$$|\phi(-t_c)\rangle = \pi^{-\frac{1}{4}} \alpha^{-1/2} \int_{-\pi}^{\pi} e^{-\frac{(k_c-k)^2}{2\alpha^2} + i(k_c-k)j_c} |k\rangle dk. \quad (39)$$

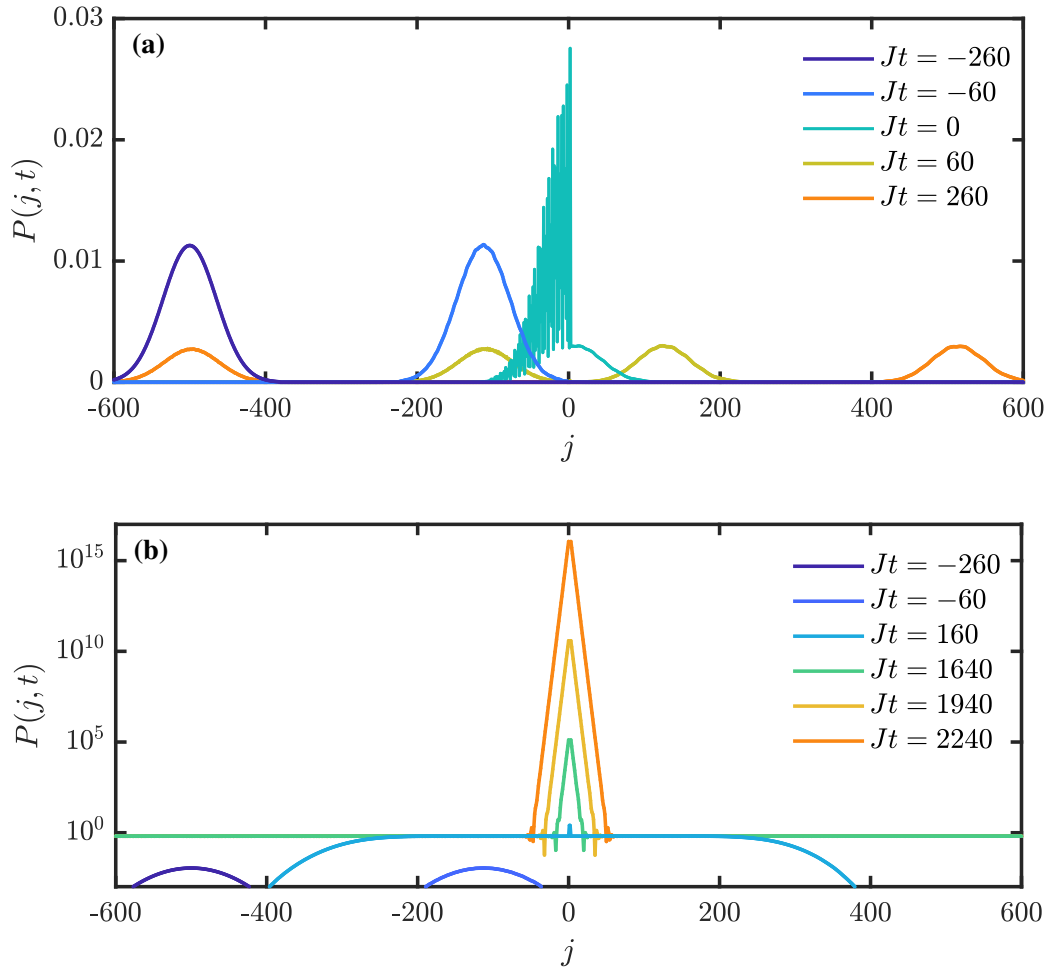


FIG. 4. Scattering of a Gaussian wave packet in the waveguide by a giant atom for (a) a loss rate $\gamma/J \approx -0.215$ and (b) a critical gain rate $\gamma/J \approx 0.215$ satisfying Eqs. (24). The incident wave packet is initially localized at $j_c = -500$ on a lattice of 10^4 sites, with mean wave number $k_c = 1.32$ and with parameter $\alpha = 0.02$. All other parameters are the same as Fig. 2 (c) and (d). The vertical scale in (b) is logarithmic.

The time evolution of the wave packet before encountering the giant atom can be expressed as

$$|\phi(t)\rangle = \pi^{-\frac{1}{4}} \alpha^{-1/2} \int_{-\pi}^{\pi} e^{-\frac{(k_c-k)^2}{2\alpha^2} + i(k_c-k)j_c} e^{-i\omega_k(t+t_c)} |k\rangle dk. \quad (40)$$

If the parameter α is small enough (here we choose $\alpha = 0.02$), the integration range in

Eq. (40) can be extended from $-\infty$ to ∞ , and the resulting probability density is [51, 52]

$$P(j, t) \approx \frac{1}{\sqrt{\pi}} \frac{1}{\sqrt{\alpha^{-2} + [\alpha\omega''_{k_c}(t + t_c)]^2}} \exp \left\{ -\frac{(j - v_c t)^2}{\alpha^{-2} + [\alpha\omega''_{k_c}(t + t_c)]^2} \right\}, \quad (41)$$

where ω''_{k_c} denotes the second derivative of the dispersion relation evaluated at k_c . The wave packet maintains the Gaussian shape with the width increasing monotonically over time, thus it spreads and the height diminishes as it propagates towards the giant atom, as shown by the $Jt = -60$ curve in Fig. 4 (a).

When the wave packet interacts with the giant atom, part of it is absorbed. The remaining portion exhibits distinct rapid oscillations arising from interference between the reflected and incident wave packets, and eventually splits into well separated reflected and transmitted components. Due to the absence of bound states in the dissipative case, the scattering can be completely described by the scattering states derived in Sec. III. In the simulation, we define the reflection and transmission probabilities by summing all probability amplitudes propagating to the left and to the right, respectively, as follows [28, 53]:

$$R_L(t) = \sum_{j<0} P(j, t), \quad T_L(t) = \sum_{j>N} P(j, t), \quad (42)$$

We check that the calculated reflection and transmission coefficients are $R_L \approx 0.245$ and $T_L \approx 0.252$ at $Jt = 260$, which agree excellently with the time-independent scattering calculations taken from Eqs. (22) and (23).

A semilogarithmic plot of the probability densities $P(j, t)$ for the critical gain case $\gamma/J \approx 0.215$ are displayed in Fig. 4 (b). We find that at early times post-scattering, such as $Jt = 160$, the profile develops a broad top-hat-like spatial distribution, a phenomenon known to occur in other systems [25, 26]. This behavior indicates the emergence of a bound state in the continuum, as we have analysed in Sec. IV. Fig. 3 shows that the mean wave number of the incoming wave packet exactly matches that of the first bound state, i.e., $k_c = k_1$. Thus, with $|C_1|^2 \gg |C_2|^2$, the probability of the first bound state greatly exceeds that of the second at the early time, making it the dominant contributor. Since the energy of the first bound state lies on the real axis, $E_1/J \approx -0.496$, and the corresponding real wave numbers is $k_1 = 1.32$, we get $P(j, t) = |\Psi_1(j, t)| \propto \text{constant}$ from Eq. (35), indicating the bidirectional outgoing plane waves.

However, the persistence of the plateau is limited in time. Since the second bound state has a positive imaginary part, $\text{Im}(E_2)/J \approx 0.021$, it undergoes sustained amplification,

leading to its eventual dominance at later times. In Fig. 4 (b), we observe that the early plateau is replaced by a sharp localized triangular peak at much later times $Jt = 1900, 2200$ and 2500 . Based on Eq. (35), we have $P(t) \propto e^{2\text{Im}(E_2)t}$, demonstrating temporal exponential growth with rate $\text{Im}(E_2)/J \approx 0.021$ shown in the center region. Similarly, it follows from the spatial decay described by $P(j) \propto e^{2\text{Im}(k_2)j}$ for $j < 0$ and $P(j) \propto e^{-2\text{Im}(k_2)j}$ for $j > N$ that the slopes on both sides of the triangular peak are in excellent agreement with twice the imaginary part of the wave number, i.e., $2\text{Im}(k_2) \approx 0.776$. These findings constitute conclusive evidence that the excitation of a time-growing bound state is the direct cause of the system's anomalous long-time behavior.

V. CONCLUSION

In this work, we have investigated the single-photon scattering in a one-dimensional coupled-resonator waveguide, mediated by a lossy or gain giant atom. This system can be modeled by a one-dimensional tight-binding chain, with the giant atom coupled to two lattice sites. To incorporate the effects of loss and gain, we extend the conventional two-level model for this giant atom by making its on-site energy complex-valued, with its imaginary part γ signifying absorption (for $\gamma < 0$) or amplification (for $\gamma > 0$). The resulting non-Hermitian Hamiltonian is treated by a correspondingly generalized projection operator formalism, which we then apply to the single-photon scattering problem.

With the scattering theory established on the analyzed scattering states, we derive the expression for the scattering matrix and then present the resulting reflection and transmission coefficients. While a lossy giant atom absorbs the incident wave, a gain giant atom not only amplifies it but can also induce divergence at specific energies, which corresponds to persistent wave emission. Solving the eigenequation of the effective Hamiltonian reveals that the divergence corresponds to a bound state embedded in the continuum. Furthermore, analysis of the energy spectrum indicates the simultaneous emergence of at least one additional bound state that exhibits temporal growth. Although the initial overlap of an incident wave packet with the time-growing bound state may be minimal, this component nevertheless experiences exponential amplification, whereby it comes to dominate the long-time evolution. We performed numerical simulations of a Gaussian wave packet propagation to verify the theoretical predictions. In particular, the appearance of the probability densi-

ties plateau and the subsequent formation of a triangular peak at long times are attributed to the characteristics of the bound states.

Crucially, we find that for $\gamma > 0$, a time-growing bound state always exists. This implies that the reflection and transmission coefficients obtained from conventional time-independent scattering methods become unphysical in this regime. A time-dependent approach is therefore required to properly analyze wave packet evolution. We believe the technique developed here can be extended to other non-Hermitian systems, with potential applications in controlling quantum emission and absorption, constructing quantum routers and sensors, and processing quantum information.

ACKNOWLEDGMENTS

We acknowledge grant support from the National Natural Science Foundation of China (Grants No. 12475024) and the Shandong Provincial Natural Science Foundation, China (Grants No. ZR2020QA079 and No. ZR2021MA081).

Appendix A: The stationary state approach

In addition to the projection operators formalism presented in the main text, the transmission and reflection coefficients can be derived directly using the stationary state solution method. Within the single-excitation subspace, the eigenstate of the system can be expressed as

$$|\Psi\rangle = \Psi(a)|a\rangle + \sum_j \Psi(j)|j\rangle, \quad (A1)$$

where $\Psi(a)$ is the atomic excitation amplitude, and $\Psi(j)$ is the probability amplitude at waveguide site j . Substituting this ansatz into the stationary Schrödinger equation and applying the boundary conditions imposed by the giant atom coupling at sites $j = 0$ and $j = N$, we obtain the following set of equations for the amplitudes:

$$\begin{cases} (\omega_k - \omega_c)\Psi(0) + J[\Psi(-1) + \Psi(1)] - g\Psi(a) = 0, \\ (\omega_k - \omega_c)\Psi(N) + J[\Psi(N-1) + \Psi(N+1)] - g\Psi(a) = 0, \\ (\omega_k - \omega_a - i\gamma)\Psi(a) - g[\Psi(0) + \Psi(N)] = 0, \end{cases} \quad (A2)$$

where $\omega_k = \omega_c - 2J \cos k$ is the waveguide dispersion. The solutions to Eqs. (A2) are plane waves, and the probability amplitude for a photon incident from the left can be considered in the form of

$$\Psi(j) = \begin{cases} Ve^{ikj} + We^{-ikj}, & j < 0, \\ Xe^{ikj} + Ye^{-ikj}, & 0 \leq j < N, \\ Ze^{ikj}, & j \geq N. \end{cases} \quad (\text{A3})$$

with $0 \leq k \leq \pi$. Together with the continuous condition at $j = 0$ and $j = N$, which are $V + W = X + Y$ and $Xe^{ikN} + Ye^{-ikN} = Ze^{ikN}$, we can solve Eq. (A2) and obtain the scattering amplitudes for $\omega_a = \omega_c$,

$$r = \frac{W}{V} = -\frac{g^2(1 + e^{ikN})^2}{2g^2(1 + e^{ikN}) - 2iJ \sin k(\omega_k - \omega - i\gamma)}, \quad (\text{A4})$$

$$t = \frac{Z}{V} = 1 + \frac{g^2(1 + e^{ikN})(1 + e^{-ikN})}{2iJ \sin k(\omega_k - \omega_a - i\gamma) - 2g^2(1 + e^{ikN})}. \quad (\text{A5})$$

One can verify that these amplitudes coincide with Eqs. (22) and (23) in the main text for $\omega_a = \omega_c$.

Appendix B: The Siegert boundary condition

When V equals zero in Eq. (A3), poles emerge in the scattering amplitudes Eqs. (22) and (23). One should apply the Siegert boundary condition to describe these non-scattering states. The Siegert boundary condition expands the discrete set of k_n to the complex plane, with associated complex energies $E_n = \omega_c - 2J \cos k_n$. The time evolution of the corresponding eigenstate is given by

$$\Psi(j, t) = e^{-iE_n t} \times \begin{cases} We^{-ik_n j}, & j < 0, \\ Xe^{ik_n j} + Ye^{-ik_n j}, & 0 \leq j < N, \\ Ze^{ik_n j}, & j \geq N. \end{cases} \quad (\text{B1})$$

The states are classified according to the position of k_n in the complex plane. k_n on the positive and negative imaginary axis correspond to bound states and virtual states, respectively. The resonant states appear in the fourth quadrant, while their antiresonant partners reside on the third quadrant. For the non-unitary cases, k_n in the first quadrant corresponds to states that norm grow exponentially with time, and k_n in the second quadrant corresponds to states that norm decreases with time. In our system, we only find k_n located

on the positive imaginary axis, the positive real axis, and in the first quadrant for outgoing wave packets.

- [1] A. Blais, A. L. Grimsmo, S. M. Girvin, and A. Wallraff, Circuit quantum electrodynamics, *Rev. Mod. Phys.* **93**, 025005 (2021).
- [2] D. Roy, C. M. Wilson, and O. Firstenberg, Colloquium: Strongly interacting photons in one-dimensional continuum, *Rev. Mod. Phys.* **89**, 021001 (2017).
- [3] H. Zheng and H. U. Baranger, Persistent quantum beats and long-distance entanglement from waveguide-mediated interactions, *Phys. Rev. Lett.* **110**, 113601 (2013).
- [4] M. Spethmann, X.-P. Zhang, J. Klinovaja, and D. Loss, Coupled superconducting spin qubits with spin-orbit interaction, *Phys. Rev. B* **106**, 115411 (2022).
- [5] A. S. Sheremet *et al.*, Waveguide quantum electrodynamics: Collective radiance and photon-photon correlations, *Phys. Rep.* **1017**, 1 (2023).
- [6] H. Xu *et al.*, Topological energy transfer in an optomechanical system with exceptional points, *Nature* **537**, 80 (2016).
- [7] U. Fano, Effects of configuration interaction on intensities and phase shifts, *Phys. Rev.* **124**, 1866 (1961).
- [8] S. S. Szigeti, O. Hosten, and S. A. Haine, Improving cold-atom sensors with quantum entanglement: Prospects and challenges, *Appl. Phys. Lett.* **118**, 140501 (2021).
- [9] B. Kannan, M. J. Ruckriegel, D. L. Campbell, *et al.*, Waveguide quantum electrodynamics with superconducting artificial giant atoms, *Nature* **583**, 775 (2020).
- [10] A. M. Vadiraj, A. Ask, T. G. McConkey, I. Nsanzineza, C. W. S. Chang, A. F. Kockum, and C. M. Wilson, Engineering the level structure of a giant artificial atom in waveguide quantum electrodynamics, *Phys. Rev. A* **103**, 023710 (2021).
- [11] W. Zhao and Z. Wang, Single-photon scattering and bound states in an atom-waveguide system with two or multiple coupling points, *Phys. Rev. A* **101**, 053855 (2020).
- [12] L. Du, M.-R. Cai, J.-H. Wu, Z. Wang, and Y. Li, Single-photon nonreciprocal excitation transfer with non-Markovian retarded effects, *Phys. Rev. A* **103**, 053701 (2021).
- [13] L. Guo, A. Grimsmo, A. F. Kockum, M. Pletyukhov, and G. Johansson, Giant acoustic atom: A single quantum system with a deterministic time delay, *Phys. Rev. A* **95**, 053821 (2017).

[14] G. Andersson, B. Suri, L. Guo, *et al.*, Non-exponential decay of a giant artificial atom, *Nat. Phys.* **15**, 1123 (2019).

[15] Q. Y. Cai and W. Z. Jia, Coherent single-photon scattering spectra for a giant-atom waveguide-QED system beyond the dipole approximation, *Phys. Rev. A* **104**, 033710 (2021).

[16] X. Wang, K.-W. Huang, and H. Xiong, Magnon blockade in a QED system with a giant spin ensemble and a giant atom coupled to a waveguide, *Phys. Rev. A* **110**, 033702 (2024).

[17] X. S. Ma, J. H. Quan, Y. N. Lu, and M.-T. Cheng, Quantum enhancement of qutrit dynamics of a three-level giant atom coupling to a one-dimensional waveguide, *Results Phys.* **56**, 107252 (2024).

[18] Z. Y. Li and H. Z. Shen, Non-Markovian dynamics with a giant atom coupled to a semi-infinite photonic waveguide, *Phys. Rev. A* **109**, 023712 (2024).

[19] S. J. Sun, Z. Y. Li, C. Cui, S. Xu, and H. Z. Shen, Non-Markovian dynamics of a driven three-level giant atom coupled to a semi-infinite waveguide via complex couplings, *Phys. Rev. A* **112**, 063704 (2025).

[20] T. Søndergaard and B. Tromborg, General theory for spontaneous emission in active dielectric microstructures: Example of a fiber amplifier, *Phys. Rev. A* **64**, 033812 (2001).

[21] A. Pick, B. Zhen, O. D. Miller, C. W. Hsu, F. Hernandez, A. W. Rodriguez, M. Soljačić, and S. G. Johnson, General theory of spontaneous emission near exceptional points, *Opt. Express* **25**, 12325 (2017).

[22] S. Franke, J. Ren, M. Richter, A. Knorr, and S. Hughes, Fermi's golden rule for spontaneous emission in absorptive and amplifying media, *Phys. Rev. Lett.* **127**, 013602 (2021).

[23] J. Ren, S. Franke, B. VanDrunen, and S. Hughes, Classical Purcell factors and spontaneous emission decay rates in a linear gain medium, *Phys. Rev. A* **109**, 013513 (2024).

[24] B. VanDrunen, J. Ren, S. Franke, and S. Hughes, Gain-modified emission dynamics between two quantum emitters in a plasmonic gain cavity system, *Phys. Rev. A* **112**, 013532 (2025).

[25] S. Longhi, Spectral singularities in a non-Hermitian Friedrichs-Fano-Anderson model, *Phys. Rev. B* **80**, 165125 (2009).

[26] P. Wang, L. Jin, G. Zhang, and Z. Song, Wave emission and absorption at spectral singularities, *Phys. Rev. A* **94**, 053834 (2016).

[27] L. Jin and Z. Song, Incident direction independent wave propagation and unidirectional lasing, *Phys. Rev. Lett.* **121**, 073901 (2018).

[28] C. Zheng, Physical relevance of time-independent scattering calculations in non-Hermitian systems: The role of time-growing bound states, *Phys. Rev. A* **112**, 042228 (2025).

[29] H. F. Jones, Scattering from localized non-Hermitian potentials, *Phys. Rev. D* **76**, 125003 (2007).

[30] S. Longhi, Spectral singularities and Bragg scattering in complex crystals, *Phys. Rev. A* **81**, 022102 (2010).

[31] A. Mostafazadeh, Semiclassical analysis of spectral singularities and their applications in optics, *Phys. Rev. A* **84**, 023809 (2011).

[32] A. Abouzaid and A. F. J. Levi, Supersymmetry with scattering states, *Europhys. Lett.* **135**, 40002 (2021).

[33] W. D. Heiss, H. Cartarius, G. Wunner, and J. Main, Spectral singularities in PT-symmetric Bose–Einstein condensates, *J. Phys. A: Math. Theor.* **46**, 275307 (2013).

[34] H. Ramezani, H.-K. Li, Y. Wang, and X. Zhang, Unidirectional spectral singularities, *Phys. Rev. Lett.* **113**, 263905 (2014).

[35] T. Liu, X. Zhu, F. Chen, S. Liang, and J. Zhu, Unidirectional wave vector manipulation in two-dimensional space with an all passive acoustic parity-time-symmetric metamaterials crystal, *Phys. Rev. Lett.* **120**, 124502 (2018).

[36] W. Wang and W. Yi, Dynamic transition of the density-matrix topology under parity-time symmetry, *Phys. Rev. B* **110**, 155141 (2024).

[37] H. C. Wu and L. Jin, Topological zero modes from the interplay of \mathcal{PT} symmetry and anti- \mathcal{PT} symmetry, *Phys. Rev. B* **112**, 125146 (2025).

[38] H. T. Dung, L. Knöll, and D.-G. Welsch, Spontaneous decay in the presence of dispersing and absorbing bodies: General theory and application to a spherical cavity, *Phys. Rev. A* **62**, 053804 (2000).

[39] C. Raabe and D.-G. Welsch, QED in arbitrary linear media: Amplifying media, *Eur. Phys. J. Spec. Top.* **160**, 371 (2008).

[40] H. Feshbach, A unified theory of nuclear reactions. II, *Ann. Phys.* **19**, 287 (1962).

[41] I. Rotter, A non-Hermitian Hamilton operator and the physics of open quantum systems, *J. Phys. A: Math. Theor.* **42**, 153001 (2009).

[42] Y. S. Greenberg and A. A. Shtygashev, Non-Hermitian Hamiltonian approach to the microwave transmission through a one-dimensional qubit chain, *Phys. Rev. A* **92**, 063835 (2015).

- [43] N. Hatano and G. Ordonez, Time-reversal symmetric resolution of unity without background integrals in open quantum systems, *J. Math. Phys.* **55**, 122106 (2014).
- [44] J. J. Sakurai and J. Napolitano, *Modern Quantum Mechanics* (Cambridge University Press, 2017).
- [45] L. Canto and M. Hussein, *Scattering Theory of Molecules, Atoms and Nuclei* (World Scientific, 2012).
- [46] S. Garmon, M. Gianfreda, and N. Hatano, Bound states, scattering states, and resonant states in \mathcal{PT} -symmetric open quantum systems, *Phys. Rev. A* **92**, 022125 (2015).
- [47] K. Sasada, N. Hatano, and G. Ordonez, Resonant spectrum analysis of the conductance of an open quantum system and three types of Fano parameter, *J. Phys. Soc. Jpn.* **80**, 104707 (2011).
- [48] N. Hatano and G. Ordonez, Time-reversal symmetric resolution of unity without background integrals in open quantum systems, *J. Math. Phys.* **55**, 122106 (2014).
- [49] A. J. F. Siegert, On the derivation of the dispersion formula for nuclear reactions, *Phys. Rev.* **56**, 750 (1939).
- [50] C. M. Bender and S. A. Orszag, *Advanced Mathematical Methods for Scientists and Engineers* (Springer, 1999).
- [51] W. Kim, L. Covaci, and F. Marsiglio, Impurity scattering of wave packets on a lattice, *Phys. Rev. B* **74**, 205120 (2006).
- [52] M. Staelens and F. Marsiglio, Scattering problems via real-time wave packet scattering, *Am. J. Phys.* **89**, 693 (2021).
- [53] Y. Chen, M. Wubs, J. Mørk, and A. F. Koenderink, Coherent single-photon absorption by single emitters coupled to one-dimensional nanophotonic waveguides, *New J. Phys.* **13**, 103010 (2011).